



## Copyright Notice

©2012 IEEE. Personal use of this material is permitted. However, permission to reprint/republish this material for advertising or promotional purposes or for creating new collective works for resale or redistribution to servers or lists, or to reuse any copyrighted component of this work in other works must be obtained from the IEEE.

This document was downloaded from Chalmers Publication Library (<http://publications.lib.chalmers.se/>), where it is available in accordance with the IEEE PSPB Operations Manual, amended 19 Nov. 2010, Sec. 8.1.9 (<http://www.ieee.org/documents/opsmanual.pdf>)

(Article begins on next page)

# Design and Experimental Validation of Cooperative Driving System in Grand Cooperative Driving Challenge

Roozbeh Kianfar\*, Bruno Augusto<sup>‡</sup>, Alireza Ebadighajari<sup>×</sup>, Usman Hakeem<sup>∇</sup>, Josef Nilsson<sup>\*,†</sup>, Ali Raza<sup>◊</sup>, Reza S Tabar<sup>×</sup>, Naga VishnuKanth Irukulapati\*, Cristofer Englund<sup>‡</sup>, Paolo Falcone\*, Stylianos Papanastasiou<sup>◊</sup>, Lennart Svensson\*, Henk Wymeersch\*

**Abstract**—In this paper we present a Cooperative Adaptive Cruise Control (CACC) architecture, proposed and implemented by the team from Chalmers University of Technology that joined the Grand Cooperative Driving Challenge (GCDC) in 2011. The proposed CACC architecture consists of three main components, namely, *communication*, *sensor fusion* and *control*, which are described in detail. Both simulation and experimental results are provided, demonstrating that the proposed CACC system is able to drive within a vehicle platoon, while minimizing the inter-vehicle spacing within the allowed range of safety distances, tracking a desired speed profile, and attenuating acceleration shockwaves.

**Index Terms**—Cooperative Driving, Multi-Vehicle Formations, Vehicle Platoons, Vehicle-to-Vehicle (V2V), Vehicle-to-Infrastructure (V2I), Automatic Control, Sensor Fusion.

## I. INTRODUCTION

ACCORDING to the ERF<sup>1</sup> - 2010 European Road Statistics report [2], the *tonne-kilometer*<sup>2</sup> on the EU-27<sup>3</sup> road network has grown by 45.6% over the period 1995-2008, with a rate of 2.9% per year. Similarly, the *passenger-kilometer*<sup>4</sup> has grown by 21.4%, with a rate of 1.5% per year. In 2008, this growth led to shares of 72.5% and 72.4% of the total inland EU-27 transportation of goods and passengers, respectively, to take place on the road network. Although the ERF document does not report detailed road congestion data, the figures in [2] motivate questioning whether the existing road network has, at the current growth rate, the capacity to meet the

future demands of road transportation (of both goods and passengers). Indeed, 53% of the 2007-2013 EU-12 structural funds are allocated for development and maintenance of the European road network.

Fortunately, building or expanding road infrastructures is not the only remedy for traffic congestion. Advances in vehicular, communication and information technologies can contribute to alleviate traffic congestion, by enabling cooperation among vehicles to better exploit the usage of the *existing* roads capacity. This idea dates back to the eighties [9], when California's Partners for Advanced Transit and Highways (PATH) program was established to study and develop vehicle-highway cooperation and communication systems [1]. The basic idea is to enable the communication and the cooperation among neighboring vehicles in order to safely reduce their mutual distance (thus leading to more vehicles without increasing the road capacity) and suppress traffic shockwaves (thus reducing pollutant emissions). The core of such cooperative driving systems is a set of algorithms, deployed on the vehicles and controlling their motion based on the behavior of the surrounding vehicles.

Low-cost and reliable communication systems have recently renewed the interest in cooperative vehicle-highway systems. In the 2011 Grand Cooperative Driving Challenge (GCDC) [3], a number of vehicles have cooperated in platoons in both urban and highway driving scenarios. The aim of the 2011 GCDC was to accelerate the development, integration, demonstration, and deployment of cooperative driving systems, based on the combination of Vehicle-to-Vehicle (V2V) and Vehicle-to-Infrastructure (V2I) communication infrastructures [3] and the state-of-the-art of sensor fusion and control. The challenge was to demonstrate how traffic shockwaves can be attenuated and the road throughput increased, i.e., the inter-vehicle spacing reduced, by (i) conveying surrounding vehicles' state and road information to each vehicle in the platoon, (ii) locally fusing the collected information into awareness of the surrounding context in order to (iii) locally control the vehicle longitudinal motion and the distance from the preceding vehicle.

In this paper, we present the cooperative driving system developed by the Chalmers' team for GCDC 2011. The system architecture is first introduced and motivated, then the three main modules accomplishing the tasks (i)-(iii) are thoroughly

\*Department of Signals and Systems, Chalmers University of Technology, SE-412 96 Göteborg, Sweden, E-mail: {roozbeh,vnaga,falcone,lennart.svensson,henkw}@chalmers.se

<sup>‡</sup>VTI Swedish National Road and Transport Research Institute, E-mail: bruno.augusto@vti.se

<sup>∇</sup>E-mail: usman.hakeem@ericsson.com

<sup>†</sup>SP Technical Research Institute of Sweden, E-mail: josef.nilsson@sp.se

<sup>◊</sup>E-mail: rali@student.chalmers.se

<sup>×</sup>Volvo Car Corporation, E-mail: rsadeghi@volvocars.com, aebadigh@volvocars.com

<sup>‡</sup>Viktoria Institute, E-mail: cristofer.englund@viktoria.se

<sup>◊</sup>E-mail: stylianos@gmail.com

<sup>1</sup>European Union Road Federation

<sup>2</sup>Tonne-kilometer (tkm) is the service of moving one ton of payload over a distance of one kilometer [4].

<sup>3</sup>27 member states European Union

<sup>4</sup>Passenger-kilometer (pkm) is the distance (km or miles) traveled by passengers on transit vehicles. This is determined by multiplying the number of unlinked passenger trips by the average length of their trips [4]



Fig. 1. Photograph of the Team Chalmers' competition vehicle during GCDC 2011.

described. Simulation and experimental results are presented showing how the proposed cooperative driving system is capable of tracking a desired speed profile, while minimizing the distance from the preceding vehicle and attenuating accelerations shockwaves.

The paper is organized as follows. Section II describes the problem and the GCDC context. Section III overviews the cooperative driving system architecture. Section IV describes the communication hardware and software, Section V and VI present the sensor fusion and control algorithms, respectively. The simulation and experimental results are presented and discussed in Section VII while Section VIII concludes the paper with final remarks.

## II. PROBLEM STATEMENT/GCDC CONTEXT

GCDC is a challenge where participants compete in cooperative driving scenarios. The scenarios are chosen to demonstrate the ability of the participating vehicles of cooperating in order to *safely* and *efficiently* drive in formation, while reducing the inter-vehicle distances. The competition took place on the A270, a public highway, between Helmond and Eindhoven in the Netherlands, that was closed for the general public during the competition. The challenge comprises eighteen heats, each consisting of an urban and a highway scenario. In each heat, the platoons compositions are altered, for the sake of fair evaluation.

In the urban and highway scenarios (see Figure 2) the vehicles have to regulate their speed to the set-points broadcasted by a leading vehicle, subject to the rules and the evaluation criteria explained in Section II-C (see Rules and Technology document [3]).

### A. Urban scenario

In the urban scenario (see Figure 2(a)), two competing platoons are split in two parts. The two parts of each platoon are standing at two red traffic lights. In front of the foremost parts of the platoons, a lead vehicle sets the pace.

The rearmost parts start driving at the green light and, after crossing a trigger line, the first parts of the platoons have a green light and the lead vehicle starts driving followed by the two foremost parts of the platoons. The two parts of each platoon then merge thus starting the *highway scenario*.

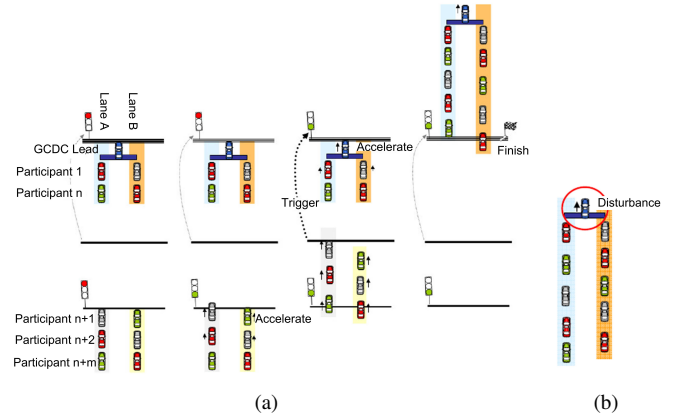


Fig. 2. Illustration of the competition scenarios [3]. The four to the left shows the sequence of the urban scenario (a). The rightmost shows the highway scenario (b).

### B. Highway scenario

In the highway scenario (see Figure 2(b)), the lead vehicle introduces acceleration disturbances, called acceleration shockwaves, by braking and accelerating. The vehicles in the platoon that crosses the finish line first receive a point. The criteria described in the next section are used to further evaluate the vehicles' performance.

### C. Evaluation criteria

The evaluation criteria are detailed in the GCDC Rules and Technology document [3] and are summarized below:

- The *platoon length*  $L_p$  as the last vehicle passes the finish line for the urban scenario.

$$L_p(t_1) = x_{\text{lead}}(t_1) - x_f, \quad (1)$$

where  $x_{\text{lead}}(t)$  is the position of the rear bumper of the GCDC lead vehicle at time  $t$ ,  $t_1$  is the time when the rear bumper of the last vehicle in the platoon passes the finish line, and  $x_f$  is the location of the finish line. The length of the vehicles is subtracted from the platoon length to compensate for the different vehicle lengths. Thus, participants are evaluated on the the platoon length expressed as the *total gap length*  $L_g$ :

$$L_g(t_1) = L_p(t_1) - \sum_{i=1}^m L_i, \quad (2)$$

where  $L_i$  is the  $i$ -th vehicle length and the vehicles are enumerated from 1 to  $m$ , with 1 and  $m$  the first and last vehicles in the platoon, respectively.

- The *maximum gap length*  $L_{g,\text{max}}$  between any two vehicles in the platoon reached during the highway scenario:

$$L_{g,\text{max}} = \max_{t \in [t_2, t_3]} \left( L_p(t) - \sum_{i=2}^m L_i \right), \quad (3)$$

where  $t_2$  and  $t_3$  denote the start and stop time of the highway scenario.

- The *platoon length variation*  $v_{LP}$  during the highway part of the competition:

$$v_{LP} = \frac{1}{t_3 - t_2} \int_{t_2}^{t_3} (L_p(t) - L_s(t))^2 dt, \quad (4)$$

where  $t_2$  and  $t_3$  indicate the start and finish time of the highway scenario, respectively, and  $L_s$  is the *safety platoon length* defined as

$$L_s(t) = \sum_{i=2}^m L_i + (m - 1) \cdot (d_0 + h \cdot v_{lead}(t)), \quad (5)$$

with  $d_0$  a constant minimum distance at the rest,  $h$  the headway time (defined later) and  $v_{lead}(t)$  the speed of the lead vehicle.

- The vehicles capability of attenuating acceleration shock-waves are evaluated through the following criterion:

$$\left\| \frac{A_i(j\omega)}{A_1(j\omega)} \right\|_{H_\infty} \leq 1, \quad (6)$$

where  $A_1(j\omega)$  and  $A_i(j\omega)$  are the Fourier transforms of the accelerations of the platoon leading vehicle and the  $i$ -th vehicle, respectively. Further details on string stability can be found in the Rules and Technology document [3].

#### D. Safety requirements

The vehicle incorporate automatic longitudinal speed control whereas the lateral movements are controlled by the human driver. To safely participate the GCDC platooning scenarios the human driver is able to interrupt the automatic controller at any time. The system may be disabled if any pedals or a dedicated emergency button is pressed. Additionally, a safety distance between vehicles must be maintained, speed limits and acceleration and deceleration requirements should be met.

The distance between the vehicles should be at least:  $d_{safety} = d_0 + h \cdot v$  where  $d_0$  refers to the minimal distance at rest,  $h$  is the minimal required headway time, and  $v$  is the speed of the host vehicle in m/s. For the GCDC 2011,  $d_0 = 10\text{m}$ ,  $h = 0.6\text{s}$ ,  $v_{max} = 80\text{km/h}$  and commanded longitudinal accelerations should be in the range  $[-4.5, 2]\text{m/s}^2$ .

### III. OVERVIEW OF THE COOPERATIVE DRIVING SYSTEM ARCHITECTURE

The architecture of the cooperative driving system proposed and developed by the Chalmers' team is sketched in Figure 3. The system has been integrated into a Volvo S60, in such a way that it replaces the vehicle's existing Adaptive Cruise Control (ACC) system. The core of the software is implemented in a dSPACE real-time hardware which interacts with vehicle and the external hardware modules.

#### A. System inputs

The required measurements are collected from three main sources namely the built-in sensors in the vehicle, additional external sensors as well as the wireless communication node.

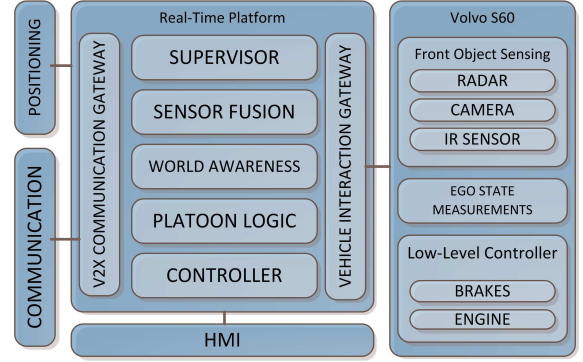


Fig. 3. A schematic overview of the developed cooperative driving system.

1) *Local, built-in sensors*: The Volvo S60 is equipped with a front object sensing module, which includes a radar, a camera, and an infra-red (IR) sensor. By fusing the measurements of these three sensors, this sensing module provides relative distance and velocity of the closest front object in the ego vehicle's path. Additionally, the built-in sensors provide ego vehicle's velocity and acceleration. These sensor measurements are acquired from the vehicle's Controller Area Network (CAN) bus.

2) *Local, added sensors*: In addition to the existing built-in sensing modules in the vehicle, a Real Time Kinematic (RTK) GPS unit was used as the positioning module. The unit outputs ego vehicle's coordinates as well as heading, velocity, and accuracy measurements. Also, Coordinated Universal Time (UTC) which is used for time synchronization in the system, is an output of this module. User Datagram Protocol (UDP) was the connection protocol of choice between the real-time hardware and the GPS unit.

3) *Communication node*: Information about the other nodes in the cooperative driving environment, i.e., other vehicles – Vehicle to Vehicle (V2V) – and road side units – Vehicle to Infrastructure (V2I) – is acquired via a wireless communication module. The received wireless messages are described in detail in [6]. The most important messages include dynamic vehicle information, e.g., velocity, acceleration, yaw rate, coordinates for each vehicle in the setup as well as platooning related information, e.g., platoon status, platoon leader ID. The RSU specific messages such as traffic light information and traffic signs are also received by the communication node. Section IV describes the implementation of the wireless communication in more detail.

#### B. System outputs

1) *Output to the vehicle's low-level controller*: On the output end, the developed system provides an acceleration command which is sent to the S60's low-level controller. The low-level controller translates the desired acceleration command into appropriate throttle and brake request. These commands are then sent to the corresponding nodes on the vehicle's CAN.

2) *Output to the communication node*: Ego vehicle’s velocity, acceleration, yaw rate along with platoon specific messages are transmitted wirelessly according to [6].

3) *Human-Machine Interface (HMI)*: For the HMI, a laptop was connected via the designated Ethernet port on a dSPACE real-time hardware. Interaction with the system and data logging was performed using a dSPACE software.

### C. Functions overview

The main software modules developed for this cooperative driving system are implemented in the real-time platform and can be defined as a set of functions as follows.

1) *Interaction gateways to external modules*: The vehicle interaction gateway acts as an interface for the vehicle’s CAN bus in order to receive the built-in sensor data and send acceleration and break requests. The V2V and V2I (V2X) communication gateway handles the UDP communication between the real-time hardware and the external communication module.

2) *Supervisor*: The supervisor block is an event based algorithm which decides on the current mode of operation for the system. This module also checks data consistency according to various operation states. The built-in safety measures in the vehicle enforce very specific course of actions for interacting with the vehicle’s actuators via CAN. The required lower-level procedures for acceleration, deceleration, braking to full-stop and resuming the motion are also managed by this block.

3) *Sensor fusion*: The output of the vehicle’s built-in front object sensing module along with the RTK GPS data and the V2V information are fed to the sensor fusion block. The three main tasks of the sensor fusion module consist of: (i) filtering the ego vehicle’s state, (ii) filtering the preceding vehicle’s state, and (iii) filtering the leader vehicle’s state. Velocity, acceleration, and position of the ego vehicle, preceding and leader vehicles are output by the sensor fusion module. Section V discusses this module in more detail.

4) *World awareness*: Identifying the preceding and leader vehicles, position and status of the traffic lights, and the speed limit at each region are outputs of the world awareness module and its sub-functions.

5) *Platoon logic*: Platooning logics such as handling join requests and ego vehicle’s platoon status are performed in the platoon logic block. Platooning operations are implemented as described in Chapter 3.6 of [6].

6) *Controller*: The controller provides the end output of the cooperative driving system which is the required acceleration command to the vehicle. Section VI describes the details of the control algorithm.

## IV. COMMUNICATION

The communication module of the cooperative driving system (see Figure 3) facilitates real-time, fail-safe, and reliable wireless V2V and V2I communications based on the IEEE 802.11p protocol. The specification of the interaction protocol [6] as well as a reference implementation of the communications stack [5] were provided by the organizing authority and were used as the basis for our module. In particular, [6]

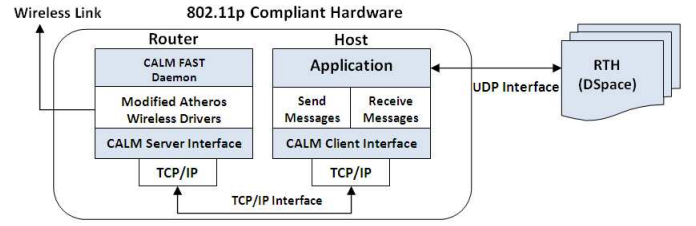


Fig. 4. Block diagram of the communication hardware interfaces.

contained in ASN.1 notation the formal syntax definition as well as the payload data structure and transmission frequency of each message type used in the competition. The communications stack [5] included modified drivers for Atheros wireless cards which allowed transmission at the appropriate frequencies as well as a user-space daemon implementing the CALM/FAST protocol. The latter is a high level protocol used on top of 802.11p for message exchange and was used by all participants as per the competition rules.

Our 802.11p based communication hardware consisted of an Alix 3D2 board containing the OpenWrt framework, an Atheros based WLAN card (Mikrotik R52H) and a 6dBi radio antenna. Note that these hardware components were provided by TNO. The CALM client interface and communication application were developed in the C programming language and the message definitions were translated to C using the open source `asn1c` compiler (v.0.9.23).

Figure 4 illustrates the block diagram of the hardware interfaces. The Alix board interfaced with real-time hardware (RTH) using a custom-designed protocol over UDP. The data received from RTH was used to generate messages in Packaged Encoding Rules (PER) unaligned format and sent over the wireless channel. Messages received over the wireless link from other entities were parsed and the extracted information was sent to the RTH which then forwarded it to other modules after having verified the data.

Two separate processes run on the board during normal operation, namely `createMessage` and `receiveMessage`; the former forwards messages to be sent wirelessly, while the latter processed received messages. Both worked independently which ensured that in case one failed, the other would continue uninterrupted whilst the failed process restarted. During block and system testing three aspects of operations were carefully monitored; round trip delay, throughput, and communication range. The tests showed an average round trip delay of 10ms at 100m line of sight (LOS) distance with no packet loss at 10Hz message frequency. In contrast, at 200m LOS distance and 200Hz message transmission frequency, a packet loss of 0.0005 was observed.

## V. SENSOR FUSION

The aim of sensor fusion is to fuse information from different sensors (listed in Section III A) to obtain a robust estimate of the state information required by the controller and other parts of the system. The sensor fusion module also makes sure that the accuracy requirements imposed by GCDC are met. A careful balance is to be taken between the information

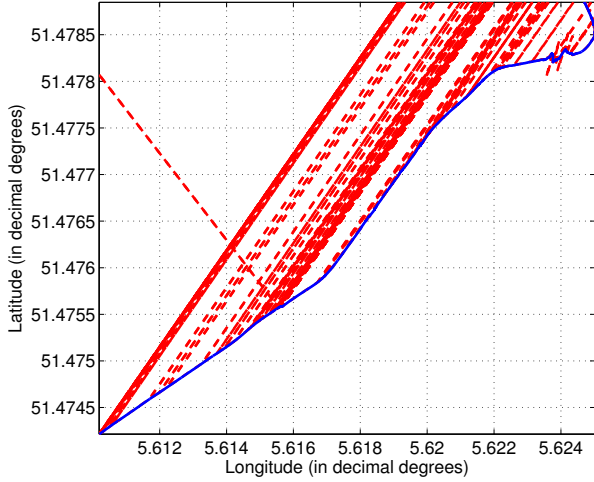


Fig. 5. Ego vehicle GPS measurement (in dashed red) and the output of the sensor fusion module (in blue). It can be seen that GPS was losing fixes very often.

from the wireless communications and in-vehicle sensors by analyzing the limitations of each sensor and complementing with other sensors.

The sensor fusion module provides filtered estimates of the state parameters of the ego vehicle, the preceding vehicle, and the leader vehicle. In filtering, the state parameters we wish to estimate can be defined in a vector that evolves over time. A filtering algorithm relies on two models: a process (or prediction) model that relates the state vector from the previous time instant to the current time instant, based on the underlying physics. Secondly, a measurement model that relates the state vector at current time to the measurements that are received at the current time. The process covariance and measurement covariance play an important role in determining the relative importance of the prediction and the measurements.

In our scenario, the state vector contains position of the ego vehicle, relative distance between the ego vehicle and the preceding vehicle, and speed and acceleration of the ego vehicle and of the preceding vehicle. Filtering is performed using the extended Kalman filter, employing a modified bicycle model as the process model. Platoon leader state estimation is based on a conventional Kalman filter. To account for delays in sensor fusion, timestamps of messages from GPS, V2V, V2I, and in-vehicle sensors are used, so that outdated data can be neglected.

During deployment, we encountered the following practical issues, which we were able to overcome by harnessing the complementary nature of the sensors:

- Information from the GPS was not reliable when the vehicle was under tunnels or bridges. In these circumstances, besides the traditional dead reckoning technique, the position of the ego vehicle is improved (see blue curve in Figure 5, showing that fusion module will take care of all the outliers in the measurements) based on the information from the front object sensing module and information from preceding vehicle.

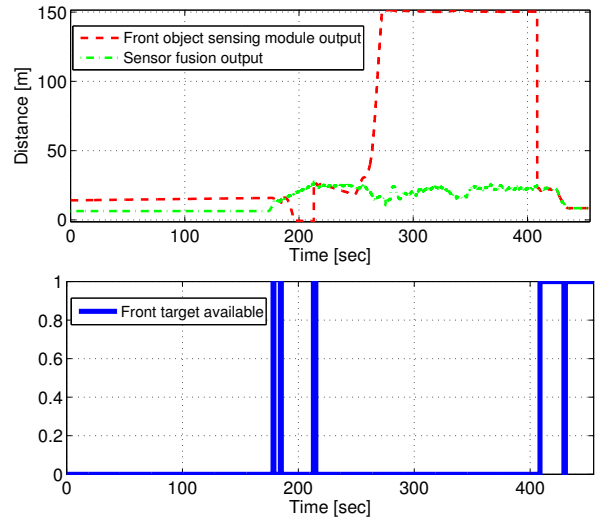


Fig. 6. Top plot shows the relative distance between the ego vehicle and the preceding vehicle as a function of time. The red curve is the output from the front object sensing module whereas the blue curve is the sensor fusion output. Bottom plot contains the 'front target available' signal sent out from Radar where it is clear that radar was not able to detect any preceding vehicle ('front target available' signal zero) most of the time due to a turning or a static vehicle in front.

- In cases of temporary target loss or invalid information from the front object sensing module, information from wireless communication was helpful. Figure 6 shows that when the front object sensing module was not giving the desired output (when the 'front target available' signal is zero), the estimation from sensor fusion module gives better result as it uses the information from other sensors.
- When there were problems with the V2V information of the preceding vehicle, the information from ego GPS and from the front object sensing module were helpful to estimate the position, speed, and acceleration of the preceding vehicle.
- The sensor fusion module also filters the signals such as acceleration and speed as seen in Figure 7.

## VI. CONTROL

In this section we present two approaches to the problem of controlling the vehicle longitudinal motion in order to achieve objectives and satisfy constraints set by the competition rules (refer to Section II). In particular, we first model the inter-vehicle spacing dynamics in Section VI-A. In Section VI-B, we state the control problem by defining control objectives and design constraints. Finally, in Section VI-C, we present a receding horizon and a frequency domain control schemes.

### A. Vehicle modeling

Consider two adjacent vehicles in Figure 8. Let  $p_i$ ,  $v_i$  and  $a_i$  denote the position, velocity and acceleration of the preceding vehicle and  $p_{i+1}$ ,  $v_{i+1}$  and  $a_{i+1}$  denote the position, velocity and acceleration of the following vehicle (the ego vehicle) in a platoon, respectively. Denote by  $e_p$  the position error w.r.t a desired distance from the preceding vehicle, i.e.,

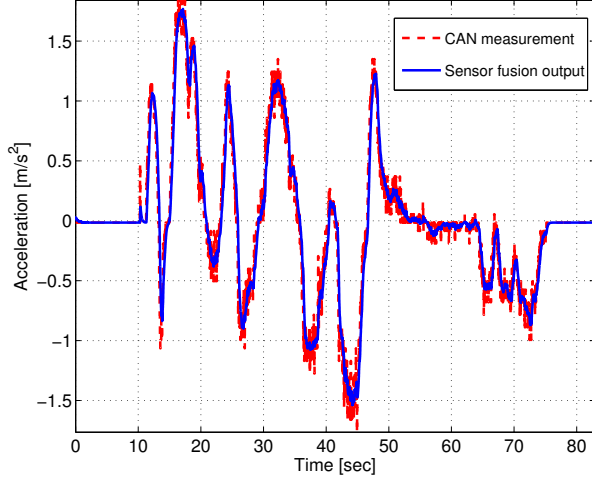


Fig. 7. Acceleration of the ego vehicle. The plot shows the measurement from the in-vehicle sensor (red curve) and the blue one is from the sensor fusion module.

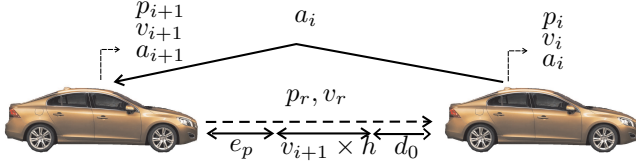


Fig. 8. Two adjacent vehicles in the platoon.

$e_p = p_i - p_{i+1} - d_0 - v_{i+1}h_{i+1}$ , where  $d_0$  and  $h_{i+1}$  are a constant safety distance and the headway time, respectively. The headway time is the time that the ego vehicle takes to reach the preceding vehicle while traveling at its current speed and is defined as

$$h_{i+1}(t) = \frac{p_i(t) - p_{i+1}(t)}{v_{i+1}(t)}. \quad (7)$$

Moreover, let  $e_v$  be the relative velocity between the two vehicles, i.e.,  $e_v = v_i - v_{i+1}$ . The error dynamics are then described by the following set of equations

$$\begin{aligned} \dot{e}_p &= e_v - a_{i+1}h_{i+1}, \\ \dot{e}_v &= a_i - a_{i+1}. \end{aligned} \quad (8)$$

The acceleration of the ego vehicle,  $a_{i+1}$  is assumed to be described by the following simplified model as follows,

$$a_{i+1} = \frac{K_{i+1}}{\tau_{i+1}s + 1} e^{-\theta s} a_{i+1}^{\text{des}}, \quad (9)$$

where  $K_{i+1}$ ,  $\tau_{i+1}$  and  $\theta$  are the steady state gain, the time constant of the actuator (engine and brake) and the actuator delay, respectively and  $a_{i+1}^{\text{des}}$  is the demanded acceleration [10]. The model (8)-(9) can then be written in the state-space form as

$$\dot{x}(t) = Ax(t) + B_1u(t - \theta) + B_2\nu(t) \quad (10)$$

where

$$A = \begin{bmatrix} 0 & 1 & -h_{i+1} & 0 \\ 0 & 0 & -1 & 0 \\ 0 & 0 & -1/\tau_{i+1} & 0 \\ 0 & 0 & 1 & 0 \end{bmatrix}, \quad (11)$$

$$B_1 = \begin{bmatrix} 0 \\ 0 \\ \frac{K_{i+1}}{\tau_{i+1}} \\ 0 \end{bmatrix}, B_2 = \begin{bmatrix} 0 \\ 1 \\ 0 \\ 0 \end{bmatrix}, \quad (12)$$

and

$$x = [e_p \quad e_v \quad a_{i+1} \quad v_{i+1}]^T, \quad (13)$$

$$u = a_{i+1}^{\text{des}}, \quad (14)$$

$$\nu = a_i, \quad (15)$$

are the state, the control and the disturbance vectors, respectively.

### B. Control problem statement and requirement satisfaction

The control objective is to minimize the position and velocity errors while satisfying a number of requirements described next.

1) *Safety*: Safety requirements are set in GCDC to guarantee that a safe *minimum* distance is maintained from the preceding vehicle in order to reduce the risk of collisions. Based on the notation introduced in Section VI-A, the safety requirements on the inter-vehicle spacing can be rewritten as

$$0 \leq e_p(t) \leq e_{p,\max}, \quad \forall t \geq 0, \quad (16)$$

where  $e_{p,\max}$  is the maximum allowed distance from the preceding vehicle. We observe that, while  $e_{p,\max}$  can be selected according to performance criteria (e.g., to not allow increasing the platoon length), the lower bound in (16) forces the distance between the ego and the preceding vehicle to be higher than  $d_0 + v_{i+1}h_{i+1}$ .

2) *Performance*: Since the primary objective of the cooperative driving system is to regulate the vehicle velocity to the platoon velocity, the relative speed between the two adjacent vehicles is constrained, i.e.,

$$e_{v,\min} \leq e_v(t) \leq e_{v,\max}, \quad \forall t \geq 0. \quad (17)$$

3) *Actuator limitations*: To ensure that the acceleration commanded by the controller is within the admissible actuator range (the controlled engine and brake), the following constraints are introduced

$$u_{\min} \leq u(t) \leq u_{\max}, \quad \forall t \geq 0. \quad (18)$$

$$\dot{u}_{\min} \leq \dot{u}(t) \leq \dot{u}_{\max}, \quad \forall t \geq 0. \quad (19)$$

4) *Desired velocity range*: To ensure that the vehicle operates within the desired velocity range which is set by the competition rules, the vehicle velocity is limited using the following constraint.

$$0 \leq v_{i+1}(t) \leq v_{\max}, \quad \forall t \geq 0, \quad (20)$$

where  $v_{\max}$  is the maximum allowed velocity.

5) *String stability*: String stability is an important property of a platoon, which refers to the capability of the vehicles in the platoon in attenuating traffic shockwaves. In general, string stability is defined w.r.t. spacing errors, that is, in a string stable platoon the spacing errors between vehicles are not amplified when propagated towards the tail of the platoon, see e.g., [7, 12]. Denote by  $e_i$  and  $e_{i+1}$  the spacing error between two adjacent vehicles, then string stability implies that

$$\left\| \frac{E_{i+1}(s)}{E_i(s)} \right\|_{\infty} \leq 1, \quad (21)$$

where  $E(s)$  is the Laplace transform of the spacing error. This definition is adopted by many researchers such as [11, 13, 12]. However, in the GCDC string stability is defined w.r.t. the vehicles accelerations

$$\left\| \frac{A_{i+1}(s)}{A_i(s)} \right\|_{\infty} \leq 1, \quad (22)$$

where  $A(s)$  is the Laplace transform of the vehicle acceleration. Such criterion is used to guarantee that the accelerations are not amplified upstream in the platoon.

### C. Controller design

In this section we present two controllers controlling longitudinal motion of the vehicle.

1) *MPC controller*: As is shown in Section VI-B, the control problem comprised multiple constraints to be satisfied. Hence, Model Predictive Control, as a powerful tool to handle constraints, can be considered as a natural choice for the controller design. In this section, we design local controllers according to a receding horizon control framework. We recall that the control objective of each vehicle is to regulate to zero the position and velocity errors  $e_p$  and  $e_v$ , respectively, while satisfying the constraints described in Section VI-B.

We assume that the state and the disturbance vectors can be measured every sampling time instant  $t_s$ , and solve the following optimization problem in receding horizon

$$\begin{aligned} \min_{\delta U_t, \varepsilon} & \sum_{k=0}^{N-1} \|y(t+k|t)\|_Q^2 + \|\delta u(t+k|t)\|_R^2 \\ & + \|u(t+k|t)\|_W^2 + \rho \varepsilon^2 \end{aligned} \quad (23)$$

subject to:

$$\begin{aligned} x(t+k+1|t) &= Fx(t+k|t) + G_1 u(t+k|t) \\ &+ G_2 \nu(t+k|t) \end{aligned} \quad (24)$$

$$y(t+k|t) = Hx(t+k|t) \quad (25)$$

$$u(t+k|t) = u(t+k-1|t) + \delta u(t+k) \quad (26)$$

$$\nu(t+k|t) = \nu(t|t) \quad (27)$$

$$k = 0, \dots, N-1$$

$$u(t-1|t) = u(t-1) \quad (28)$$

$$\nu(t|t) = \nu(t) \quad (29)$$

$$x(t|t) = x(t) \quad (30)$$

$$x_{\min}(t) - \varepsilon \leq x(t+k|t) \leq x_{\max}(t) + \varepsilon \quad (31)$$

$$u_{\min} \leq u(t+k|t) \leq u_{\max} \quad (32)$$

$$\delta u_{\min} \leq \delta u(t+k|t) \leq \delta u_{\max} \quad (33)$$

$$k = 0, \dots, N-1$$

$$\varepsilon \geq 0, \quad (34)$$

where  $\delta U_t = [\delta u(t), \dots, \delta u(t+N-1)]$  is the vector of future input increments, i.e., the vector of optimization variables,  $N$  is the prediction horizon length,  $\varepsilon$  is a slack variable introduced to soften the constraints (31),  $Q \succeq 0$ ,  $R \succ 0$  and  $W \succeq 0$  are weighting matrices of appropriate dimensions,  $\rho > 0$  penalizes the slack variable, and  $y = [e_p, e_v]^T$  is the output vector. The matrices  $F$ ,  $G_1$  and  $G_2$  are obtained by discretizing the system (10) with a sampling time  $t_s$ . Constraints (31) include the *safety* and the *performance* constraints (16)-(17), respectively, introduced in Section VI-B, while constraints (32) account for *actuators limitations*. Finally, constraints (33) guarantee *passengers comfort*.

Next we discuss how to modify the problem (23)-(34) in order to enforce string stability.

The string stability criterion (22) is defined in the frequency domain. However, for the distributed MPC scheme considered in this paper, a time domain criterion is needed. A straightforward definition of string stability in the time domain follows.

*Definition 1 (String stability)*: A vehicle platoon is string stable if for a step change in the velocity of the leader vehicle  $v_1(t)$  at time  $t = 0$ , there exist constant scalars  $\gamma_i \in (0, 1)$ ,  $i = 2, \dots, N$  such that,

$$\max_{t \geq 0} |a_{i+1}(t)| \leq \gamma_i \max_{t \geq 0} |a_i(t)|, \quad i = 2, \dots, N-1. \quad (35)$$

The condition (35) states that, in a speed change maneuver of the leader, the acceleration response of each vehicle in a string stable platoon should not exceed the acceleration of the preceding vehicle. Local controllers have then to be designed such that the (35) holds. In the distributed receding horizon framework considered in this paper, additional constraints are included in the local controller to enforce (35). Formulating general local constraints rigorously guaranteeing the (35) is not trivial. In this paper we present a practical way to enforce the attenuation of the acceleration signals. We observe that in a speed change, each vehicle in the platoon should mimic the behavior of the preceding with a delay. Hence, the following constraints can be added to the problem (23)-(33)

$$a_{i+1}(t|t_k) \leq \gamma \max_{\tau \in [t_k - H, t_k]} |a_i(\tau)| \quad \text{for } t \in [t_k, t_k + N], \quad (36)$$

where  $t_k$ , is the time instant when the optimal control signal is calculated,  $N$  is the prediction horizon length and  $H$  is the size of time window, which is a tuning parameter. The condition (36) means that at every time instant  $t_k$  the acceleration of the ego vehicle is bounded by the maximum value of the acceleration profile of the preceding, over a past time interval of length  $H$ . Hence, the parameter  $H$  must be chosen long enough in order to account for the delay arising from different dynamics within the platoon.

2) *Linear controller*: In this section, a controller is designed in the frequency domain, in order to regulate to zero the position and velocity errors, while satisfying the string stability requirement (22).

The control law  $u(t)$  is an output feedback controller with the following structure

$$u(t) = K_c \varepsilon(t) \quad (37)$$

where  $K_c = [k_p, k_v, k_a]^T$  and  $\varepsilon = [e_p, e_v, e_a]^T$  are the output feedback gain and the output vector, respectively.  $e_p$  and  $e_v$  have been defined in Section VI-A, while  $e_a$  is the relative acceleration, i.e.,  $e_a = a_i - a_{i+1}$ . The control structure is shown in Figure 9. The transfer function from the acceleration of preceding vehicle to the acceleration of the ego vehicle is

$$\Gamma(s) = \frac{A_{i+1}(s)}{A_i(s)} = \quad (38)$$

$$\frac{s^2 k_a(s)P(s) + s k_v(s)P(s) + k_p(s)P(s)}{s^2(1 + k_a(s)P(s)) + s(k_v(s)P(s) + h k_p(s)P(s)) + k_p(s)P(s)}$$

where  $P(s)$  is the transfer function of (9) where the time delay is approximated using a second order Padé approximation. The controller gains in (37) are chosen such that

$$\|\Gamma(s)\|_\infty < 1, \quad (39)$$

i.e., in order to enforce string stability.

## VII. RESULTS

The cooperative driving system overviewed in Section III and detailed in Sections IV-VI has been validated through simulations and experiments. In particular, sensor fusion and control algorithms only have been validated in simulation, while the whole system has been tested in experiments.

To facilitate the comparison between the controllers presented in Sections VI-C1 and VI-C2, simulations of the two controllers use the same acceleration profile for the leader. However, the experimental setup was not the same for the two controllers but data sets were selected to illustrate similar scenarios.

This section begins with presenting simulations results before detailing the experimental setup and ending with experimental results.

### A. Vehicle model identification

The parameters in model (9) have been estimated based on experimental data collected in both driving and braking maneuvers. In driving maneuvers the following parameters have been estimated  $\theta_{ac} \simeq 0.25s$ ,  $K \simeq 1$  and  $\tau \simeq 0.45s$ . In

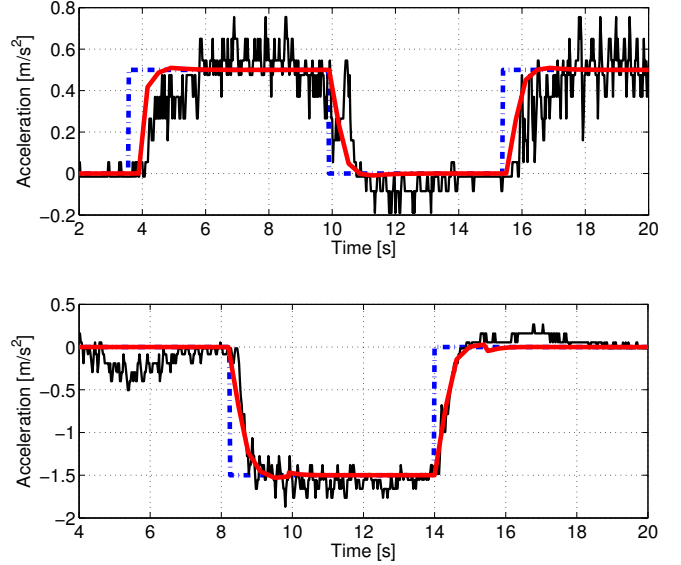


Fig. 10. Acceleration response of Volvo S60 to the commanded acceleration and output of model. The blue dashed dotted lines, the black curves and the solid red curves are the commanded acceleration, vehicle acceleration (measurement) and the output of model, respectively.

braking maneuvers, the same values for  $\tau$  and  $K$  have been found, while  $\theta_{br} \simeq 0.15s$ . Validation results of the identified model are shown in Figure 10. However, for the sake of simplicity and to avoid dealing with hybrid system, the model with shorter delay is chosen in our controller design.

### B. Simulation results

Simulations were prepared and performed using MATLAB/Simulink together with the PreScan development tool for automotive applications [8, 14]. The PreScan tool supported the inclusion of wireless communication and in-vehicle sensors and also provides an environment to configure driving scenarios.

The simulation setup consisted of a scenario with two vehicles with the preceding in first position and the ego vehicle in second position. The ego vehicle was modeled according to the parameters of the Volvo S60 presented in Section VII-A. The ego vehicles accessed the same set of sensor values as expected in a competition car. The behaviour of the leader vehicle was predefined according to an acceleration profile set up to match the competition scenarios.

Results concerning acceleration, velocity, and position error are presented in Figure 11a-f for both MPC and linear controller. Both controllers tracked a desired inter-vehicle distance determined by the minimum distance,  $d = 10m$ , and headway time,  $h = 1s$ . Additionally, constraints for the MPC are set to  $e_{p,\min} = 0$ ,  $e_{p,\max} = 3m$ ,  $e_{v,\min} = -3m/s$ ,  $e_{v,\max} = 3m/s$ ,  $u_{\min} = -4.5m/s^2$ ,  $u_{\max} = 2m/s^2$ ,  $\dot{u}_{\min} = -3m/s^3$ , and  $\dot{u}_{\max} = 3m/s^3$ .

The prediction horizon, control horizon, and sampling time for MPC control are set to  $H_p = 10$ ,  $H_c = 5$  and  $t_s = 0.1s$ , respectively. Simulations are performed by using the Model

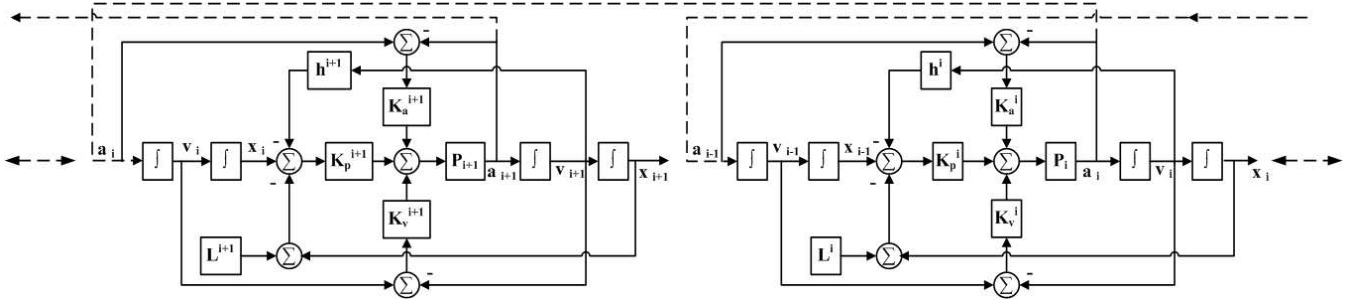


Fig. 9. Control Architecture for the heterogeneous platoon using Linear Controller.  $K_a^i$ ,  $K_v^i$  and  $K_p^i$  are the controller gain on the acceleration error, velocity error and position error of  $i^{th}$  vehicle, respectively.  $P_i$ ,  $P_{i+1}$  and  $\dots$  are the plant dynamics of different vehicles within the platoon.  $L^i$ ,  $h^i$ ,  $L^{i+1}$  and  $h^{i+1}$  are the constant safety distance and headway time for vehicle  $i$  and vehicle  $(i + 1)$ , respectively.

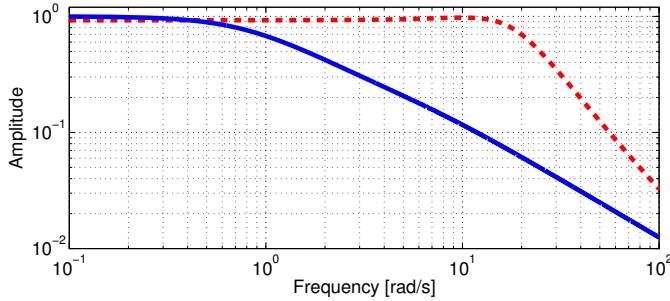


Fig. 12. Magnitude plot of transfer functions for acceleration from preceding to ego vehicle. The blue solid line is for linear controller and red dashed line is for MPC.

predictive Control Toolbox in Matlab and Simulink. Acceleration profiles shown in Figure 11a for the linear controller and in Figure 11d for the MPC both show attenuation of high frequency changes. Both controllers demonstrate smooth tracking of leader acceleration and velocity while maintaining small fluctuations around the target distance. A noticeable difference between the two controllers is the smaller position error for the linear controller. However, both acceleration and velocity tracking performance is superior for the MPC. Part of the cause for the difference can be traced back to the weighting matrices of the MPC's cost function, favoring acceleration and velocity tracking at the cost of a larger position error.

As discussed earlier, the concept of string stability was one of the main design criteria for the controllers. Figure 12 and 13 illustrate this property in the frequency and time domain, respectively. In Figure 13 (time domain) it is possible to see a platoon of six vehicles using the developed controllers. It is observed that no vehicle amplifies the acceleration of the preceding. These conclusions are confirmed by the representation in the frequency domain where the maximum amplitude of the transfer function between the ego vehicle and the preceding vehicle accelerations is less than or close to one (see Figure 12). It should be noted that in Figure 12, for the linear controller, the transfer function (38) is shown, whereas for the MPC controller, the figure shows an empirical ARX (autoregressive with exogenous terms) model identified between the acceleration of preceding and ego vehicle.

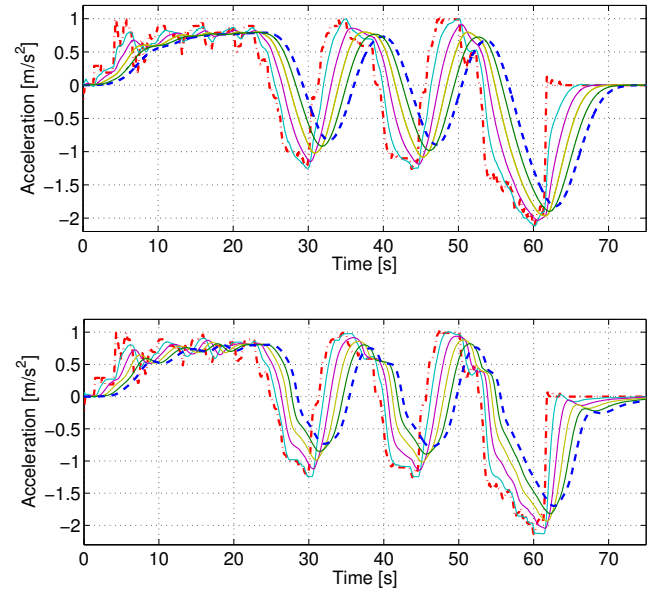


Fig. 13. Simulation results showing accelerations of each vehicle in a platoons of 6 where all vehicles use identical controllers. In the top figure all vehicles use the linear controller and in the bottom figure all vehicles use the MPC. The following line style and color schema is used in the plots: Leader vehicle (dash-dotted red line), vehicles in position two to five in the platoon (solid lines), ego vehicle (dashed blue line).

1) *Constraint satisfaction*: As it was shown in the previous section, both MPC and classical controller show satisfactory performance while perfect measurement is available and the vehicles are operating far from their constraints. However, as mentioned in Section VI-B, the control problem consists of a number of constraints to be fulfilled. Here, a harsher maneuver in presence of imperfect measurement is considered and the performance of both controllers is evaluated in terms of constraint satisfaction. Hence, the maneuver starts with acceleration, followed by deceleration, and ends up with an emergency braking. The classical controller is tuned such that it minimizes the position error and for the MPC controller the constraints on the position error are set such that,  $0[m] \leq e_p \leq 3[m]$ . The simulation results in Figure 14 show that, in the emergency braking, classical controller is violating the lower

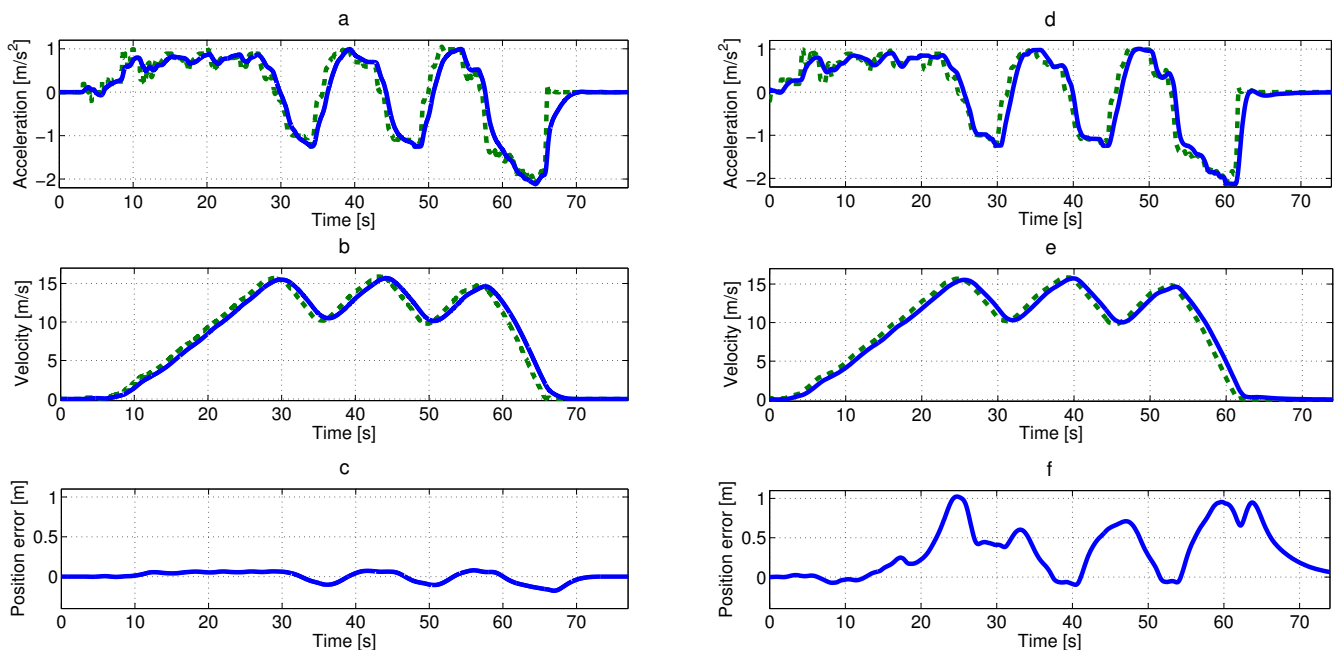


Fig. 11. Simulation results showing acceleration profiles for leader and ego vehicle for linear controller (a), acceleration profiles for leader and ego vehicle for MPC (d), velocity profiles for leader and ego vehicle for linear controller (b), velocity profiles for leader and ego vehicle for MPC (e), position error of ego relative leader vehicle for linear controller (c), and position error of ego relative leader vehicle for MPC (f). The following line style and color schema is used in the plots: Leader vehicle (dashed green line), and ego vehicle (solid blue line)

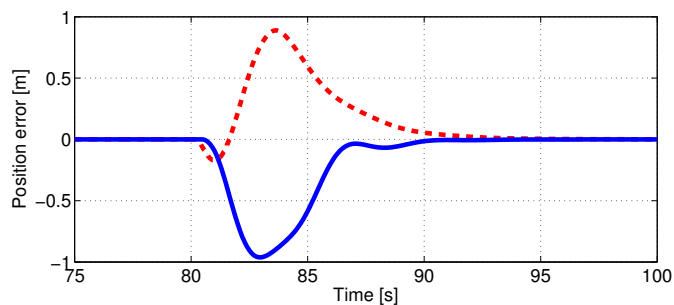


Fig. 14. Simulation results showing performance of the two controllers relative the safety distance in an emergency braking situation. The blue solid line is for linear controller and red dashed line is for MPC.

bound on the position error,  $e_p$ , while the MPC controller try to respect the constraint by avoiding negative errors. As mentioned earlier, negative position error means violating the safety distance. It should also note that, this situation is also observed in the experiment in Figure 18.

**Remark:** In the GCDC competition, the safety distance is evaluated base on the headway time  $h = 0.6s$ . Therefore, to avoid any violation of this rule, the designed controllers adopts slightly bigger headway time.

### C. Experimental results

1) *Experimental setup:* The MPC controller was experimentally tested on a 500m straight test-track road in Sweden, whereas the results for the linear controller were collected during the GCDC competition in The Netherlands. Both controllers were evaluated using the same equipment and



Fig. 15. Equipment used in the experimental setup including units for the real-time platform, positioning, wireless communication, local ethernet network, and power supply.

system configuration as described in Section III. Except for an operator laptop next to the driver, all of the equipment was placed firmly in the boot of the Volvo S60, see Figure 15.

Experiments with the MPC were initiated at standstill with vehicles lined up in a platoon formation and the ego vehicle in second place behind the leader. At start of the experiment the leader vehicle accelerated to a given speed followed by a set of brake and acceleration maneuvers before returning to standstill, see Figure 16d.

Results for the linear controller are from the urban scenario of the GCDC competition where speeds range from close to zero up to 80km/h. However, due to limited available space for

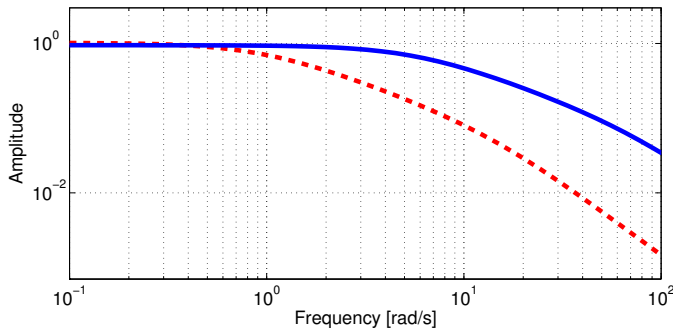


Fig. 17. Magnitude plot of transfer functions identified from experimental data. The blue solid line is for linear controller and red dashed line is for MPC.

figures and to facilitate comparison with the MPC controller, a 100s time interval was extracted from the complete data set to illustrate controller performance. The leader vehicle, as it is presented in the results of the linear controller, refer to the contestant driving one position ahead in the platoon.

2) *Results* : Results from experiments with both the linear controller and the MPC are presented in Figure 16a-f. Both controllers track a desired inter-vehicle distance determined by the minimum distance,  $d = 10m$ , and headway time,  $h = 0.85s$ . Additionally, constraints for the MPC are set to  $e_{p,\min} = 0$ ,  $e_{p,\max} = 8m$ ,  $e_{v,\min} = -4m/s$ ,  $e_{v,\max} = 4m/s$ ,  $u_{\min} = -4.5m/s^2$ ,  $u_{\max} = 2m/s^2$ ,  $\dot{u}_{\min} = 3m/s^3$ , and  $\dot{u}_{\max} = -3m/s^3$ . In comparison to the simulation results, overall the experiments yield similar performance. Tracking of both velocity and acceleration relative to the leader is achieved while keeping close to the desired inter-vehicle distance. However, some performance penalties are expected due to approximations in the vehicle model and non-optimal values of tuning variables. An observable artifact is seen 32s into the acceleration plot for the MPC, where acceleration stabilizes unreasonably lower than the leader, ensuring string-stability but allowing both velocity and position errors to grow, see Figure 16d. Notice the position error at the start of the experiment with the MPC in Figure 16f. This error, which is a result of initial positioning of the vehicles on the test-track, demonstrates how the controller corrects the distance as the experiment progresses. The correction is clearly shown for accelerations in Figure 16d from 5s to 10s into the experiment.

For evaluation of string-stability, transfer functions from preceding vehicle acceleration to ego vehicle acceleration were identified for each controller based on a second order ARX model. A magnitude plot with the two transfer functions is presented in Figure 17 showing acceleration gains from preceding to ego vehicle. As the figure illustrates, both controllers attenuate acceleration over the complete frequency spectrum. Figure 18 shows the controllers performances in the full stop. As can be seen, linear controller violates the lower bound on the position error while MPC controller regulate the error to zero.

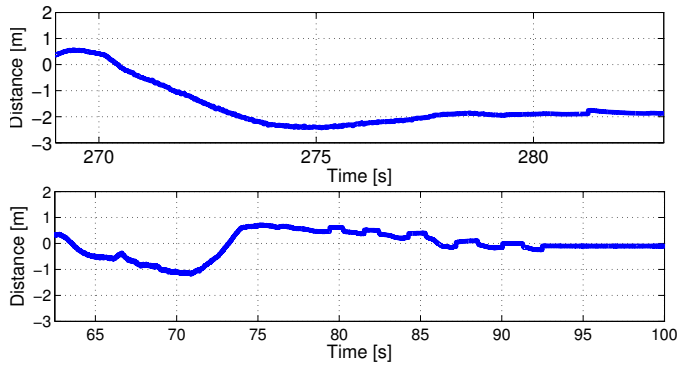


Fig. 18. Experiment results showing performance of the two controllers in regulating the position error, when the preceding vehicle brakes to a stand still. Top figure present performance of the linear controller and the bottom figure present the MPC. The preceding vehicle apply similar accelerations in both experiments.

## VIII. CONCLUSIONS

A cooperative adaptive cruise controller was presented. The system incorporates a real time, fail-safe reliable wireless communication, a RTK GPS receiver to achieve centimeter position accuracy, a rules and logic module to handle platooning events, functions to handle targets from the in-vehicle radar, camera and lidar sensors, and a sensor fusion algorithm that supplies robust signals to the controller. Communication software was successfully implemented on custom based TNO hardware and it satisfied the requirements laid down by GCDC 2011 organization, i.e., round trip delay, packet loss ratio, communication range and use of calm stack protocol. The sensor fusion system, along with other blocks in the project, was tested in real time for the GCDC competition and the results indicate that the sensor fusion system meets the GCDC requirements. We have shown during simulation and experiments that both linear and model predictive controller are string stable, i.e., attenuate high frequencies that result in dampening shock waves. Both controllers also show smooth tracking of both acceleration and velocity while maintaining a small position error. We have shown experimentally that the proposed technique is able to automatically control the vehicle while following the preceding vehicles in a platoon. Simulation and experimental results show that model predictive control is a superior approach in terms of constraint satisfaction. However, it is easier to design a string-stable platoon using linear controller, since the design procedure is more straightforward in the frequency domain. At the end, since MPC design involve more parameters which require more time to design and also due to the time constraint for the competition, the linear controller was used in the competition.

## IX. ACKNOWLEDGMENTS

This work has been carried out at SAFER - Vehicle and Traffic Safety Centre at Chalmers, Sweden and funded by the Swedish Transport Administration within the IVSS programme under contract TRV2010/55777, CoAct. We gratefully acknowledge Mark Van Der Linden (TU Eindhoven) for his support with traffic simulations.

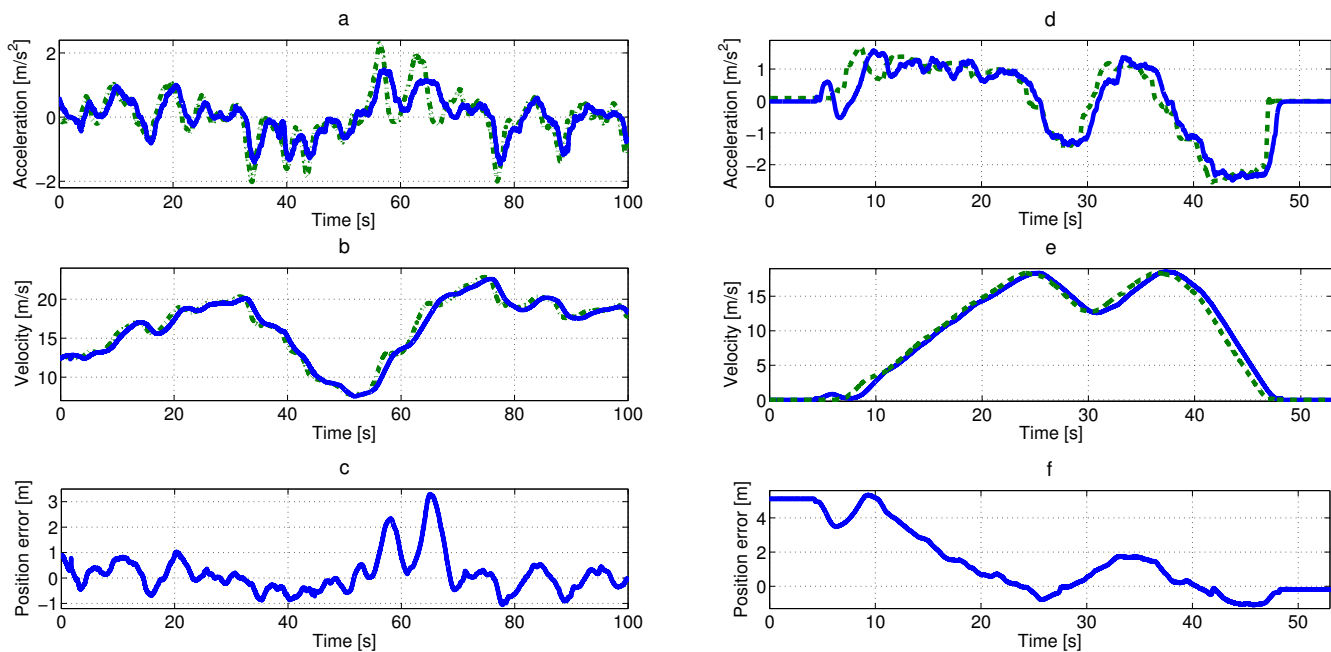


Fig. 16. Experiment results showing acceleration profiles for leader and ego vehicle with linear controller (a), acceleration profiles for leader and ego vehicle with MPC (d), velocity profiles for leader and ego vehicle for linear controller (b), velocity profiles for leader and ego vehicle for MPC (e), position error of ego relative to the leader vehicle for linear controller (c), and position error of ego relative to the leader vehicle for linear controller (f). The following color schema is used in the plots: Leader vehicle (dashed green line), and ego vehicle (solid blue line).

## REFERENCES

- [1] California Partners for Advanced Transportation Technology (PATH). <http://www.path.berkeley.edu>.
- [2] ERF 2010 European Road Statistics. [www.erf.be](http://www.erf.be).
- [3] Grand Cooperative Driving Challenge (GCDC). <http://www.gcdc.net/>.
- [4] Units of transportation measurement. [http://en.wikipedia.org/wiki/Units\\_of\\_transportation\\_measurement#Units\\_of\\_Transportation\\_Density](http://en.wikipedia.org/wiki/Units_of_transportation_measurement#Units_of_Transportation_Density).
- [5] <http://www.gcdc.net>. *GCDCCommStackV3-openwrt-gcdc*. Helmond, Netherland, 2011.
- [6] <http://www.gcdc.net>. *Interaction Protocol 2.4*. Helmond, Netherland, 2011.
- [7] M. E. Khatir and E. J. Davison. Decentralized control of a large platoon of vehicles using non-identical controllers. In *American Control Conference*, Boston, Massachusetts, USA, 2004.
- [8] MathWorks. MATLAB/Simulink. <http://www.mathworks.se/products/simulink/>, 2011.
- [9] R. M. Murray. Recent research in cooperative control of multivehicle systems. *ASME Journal of Dynamic Systems, Measurement, and Control*, 129(5):571–584, September 2007.
- [10] R. Rajamani. *Vehicle Dynamics and Control*. Springer, 2005.
- [11] P. Seiler, A. Pant, and K. Hedrick. Disturbance propagation in vehicle strings. *IEEE Transactions on automatic control*, 49(10):1835–1841, 2004.
- [12] E. Shaw and J. Karl Hedrick. Controller design for string stable heterogeneous vehicle strings. In *Proc. 46th IEEE Conf. on Decision and Control*, 2007.
- [13] Elaine Shaw and J. Karl Hedrick. Controller design for string stable heterogeneous vehicle strings. *2007 46th IEEE Conference on Decision and Control*, pages 2868–2875, 2007.
- [14] TNO. PreScan. <http://www.tno.nl/prescan>, 2011.



**Roozbeh Kianfar.** Roozbeh Kianfar received his M.S. degree in Systems, Control and Mechatronics from Chalmers University of Technology. Since 2009 he is pursuing the Ph.D degree in Mechatronics at Chalmers University of Technology. His research interests involve Model Predictive Control and its application in platooning and cooperative driving.



**Bruno Augusto.** Bruno Augusto received his M.S. in Mechanical Engineering in 2009 from Instituto Superior Técnico, Portugal. He works for the Swedish National Road and Transport Research Institute since march of 2011. Prior to that he was employed at Chalmers University of Technology where he participated in the COACT project. His interests revolve around driving simulation, active safety systems as well as vehicle dynamics control.



**Alireza Ebadighajari.** Alireza Ebadighajari received his Master degree from Chalmers University in Sweden in the field of Systems, Control and Mechatronics and his Bachelor degree from University of Tehran in the field of Electrical Engineering. Since August 2011, he is working at the Active Safety and Chassis R&D department within Volvo Cars Corporation and his areas of research interest lies within Control Theory, Autonomous Driving and Cooperative Driving fields.



**Usman Hakeem.** Usman Hakeem received his Bachelors degree in Computer Engineering from University of Engineering and Technology Taxila Pakistan. Since 2009 he is pursuing the M.S. degree in Communication Engineering at Chalmers University of Technology. Currently he is employed at Ericsson Research, department Visual Technology in Kista, Stockholm. His research areas include vehicular communication and software development in the field of video codecs.



**Josef Nilsson.** Josef Nilsson received his M.S. degree in Electrical Engineering from Chalmers University of Technology in 2007. Since 2008 he is pursuing the Ph. D. degree in Mechatronics at Chalmers University of Technology. He is currently with the Electronics department at SP Technical Research Institute of Sweden and his current research interests involve dependability of automotive applications, autonomous driving, and cooperative systems.



**Ali Raza.** Ali Raza received his M.S. degree in Communication Engineering from Chalmers University of Technology in 2011. Currently, he is working as Baseband communication engineer at Tieto Sweden AB. His work area includes design, optimization and implementation of embedded real-time systems, mainly within the telecom industry and on DSP target.



**Reza S Tabar.** Reza is currently at the conclusion of his studies towards a MSc. degree in Systems, Control and Mechatronics at Chalmers University of Technology. Since July 2011, he is working at the department of Active Safety and Chassis at Volvo Car Corporation. His main research interests are in the field of cooperative autonomous driving and vehicle active safety systems.



**Naga VishnuKanth Irukulapati.** Naga VishnuKanth Irukulapati received his B.Tech. degree in 2009 from DA-IICT, India and MSc. degree in 2011 from Chalmers University of Technology. Currently he is pursuing Ph.D in communication systems and information theory group at Chalmers University of Technology. His research interests include digital signal processing (DSP) and communication theory in general. His specific interests are in sensor fusion, DSP for wireless and fiber optical communications.



**Cristofer Englund.** Cristofer Englund received a B.Sc. degree in Electrical Engineering 2001 and a M.Sc. in Computer Science in 2003 both from Halmstad University. In 2007 he received his Ph.D. in Electrical Engineering from Chalmers Technical University. He currently holds a research manager position in the Cooperative Systems group at Viktoria Institute in Gothenburg. He is also leader of the Traffic Systems competence group at SAFER, Vehicle and Traffic Safety Centre at Chalmers. His research interests are artificial neural networks, kernel methods, pattern recognition and image processing.



**Paolo Falcone.** Paolo Falcone received the "Laurea" degree in Computer Science Engineering in 2003 from the Università di Napoli Federico II, Italy. In 2007 he received the Ph. D. degree in Automatic Control from the Dipartimento di Ingegneria at Università del Sannio, Benevento, Italy. Since April 2008 he is Assistant Professor in Mechatronics at the Department of Signals and Systems of the Chalmers University of Technology in Gothenburg, Sweden. His research interests include constrained optimal control, real-time model predictive control for fast vehicle dynamics control, active safety systems.



**Stylianos Papanastasiou.** Stylianos Papanastasiou received his combined B.Sc. degree in Computing Science and Mathematics from the University of Glasgow, UK in 2002. He was subsequently awarded his Ph.D. degree in 2006 from the Department of Computing Science at the University of Glasgow for his work titled "Investigating TCP Performance in Mobile Ad Hoc Networks". Since November 2008 he has been working as a PostDoc at Chalmers University, Sweden in the area of vehicular communications and network simulations. He has published several peer-reviewed journal and conference papers as well as a number of book chapters on the topic of ad hoc and vehicular communications. His current research interests include networking protocol analysis, and the development of precise simulators for vehicular networks.



**Lennart Svensson** Lennart Svensson was born in Älvängen, Sweden in 1976. He received the M.S. degree in electrical engineering in 1999 and the Ph.D. degree in 2004, both from Chalmers University of Technology, Gothenburg, Sweden. He is currently Associate Professor at the Signal Processing group, again at Chalmers University of Technology. His research interests include Bayesian inference in general, and nonlinear filtering and tracking in particular.



**Henk Wymeersch** (S'99, M'05) received the Ph.D. degree in Electrical Engineering/Applied sciences in 2005 from Ghent University, Belgium. He is currently an Assistant Professor with the Department of Signals and Systems at Chalmers University of Technology, Sweden. He is also affiliated with the FORCE research center on fiber-optic communication. Prior to joining Chalmers, he was a Postdoctoral Associate with the Laboratory for Information and Decision Systems (LIDS) at the Massachusetts Institute of Technology (MIT). He is a member of the IEEE, Associate Editor for IEEE Communication Letters and the European Transactions on Telecommunication (ETT). He served as Guest Editor for EURASIP Journal on Wireless Communications and Networking (special issue on Localization in Mobile Wireless and Sensor Networks) and is the author of Iterative Receiver Design (Cambridge University Press, August 2007). His research interests include algorithm design for wireless transmission, statistical inference and iterative processing.